Preprints of the 21st IFAC World Congress (Virtual)
Berlin, Germany, July 12-17, 2020

# Bilateral telemanipulation of unknown objects using remote dexterous in-hand manipulation strategies ⋆

**Andrés Montaño** * **Raúl Suárez** * **Carlos I. Aldana** **
**Emmanuel Nuño** **

* *Institute of Industrial and Control Engineering (IOC), Universitat Politècnica de Catalunya (UPC), Barcelona, Spain*
** *University Center for Exact Sciences and Engineering (CUCEI), University of Guadalajara (UDG), Guadalajara, Mexico*
*e-mails: raul.suarez@upc.edu, emmanuel.nuno@cucei.udg.mx*

**Abstract:** This paper presents an approach to perform bilateral in-hand (dexterous) telemanipulation of unknown objects. The proposed approach addresses three of the main problems in telemanipulation: kinematic issues due to the physical differences between the robotic and the human hands; obtaining coherent haptic feedback to provide information about the manipulation at any time; and time-delays that can affect the stability of the overall closed-loop system. The novelty of the approach lays on the shared control scheme, where the robotic hand uses the tactile and the kinematic information to manipulate an unknown object while the operator commands a desired orientation of the object without caring about the relation between her/his commands and the actual hand movements. The viability of the proposed approach has been tested through transatlantic telemanipulation experiments between Mexico and Spain.

*Keywords:* Robotics, telemanipulation, robot control, tactile sensors, grasping, time-delay.

## 1. INTRODUCTION

Usually, "telemanipulation" is used to refer to the teleoperation of a robot to "manipulate" objects, either joint-to-joint or end-effector to end-effector, meaning that the robot grasps and moves an object to another pose in the workspace or just with respect to the hand. In this work we use "telemanipulation" to refer to the particular case in which a robotic hand is bilaterally teleoperated to perform in-hand manipulation, also known as dexterous manipulation, i.e., moving the object using only the fingers of the hand without caring about the arm movements.

Performing dexterous telemanipulation by commanding each joint of a robotic hand as a function of each joint of the human operator hand is a complex problem. Such complexity is mainly due to: a) the kinematics of the robotic and the human hands are not fully coincident, which easily generates differences in the fingertip positions during the manipulation that may produce the loss of contacts on the object and, therefore, the object might fall; b) even when there exist several proposals, up to our knowledge, there is not any practical device that allows haptic feedback with enough precision at the level of finger joints, thus it is difficult for the operator to feel (in real practical situations) the precise state of the real grasping forces and, therefore, how critical the grasp is at any time; and c) time-delays are ubiquitous in these telemanipulation scenarios and they affect the stability of the overall closed-loop system.

In this scenario we find useful the idea of telecommanding the remote robotic hand using high level commands to autonomously perform the object manipulation within some security margins, while providing the human operator with a sense of the general state of the manipulation via haptic feedback.

This work presents a new proposal to perform "bilateral in-hand (dexterous) manipulation" using a shared control system such that the contact information is processed by the robot software in the remote station and the operator receives haptic information regarding the evolution of the object movement. Moreover, no object model is considered in the in-hand manipulation, which is equivalent to consider that the object is unknown. This strongly simplifies the human operator information regarding the object properties, even when she/he may have visual feedback of the remote scene. Furthermore, real experimentation has been done to show the viability of the proposal, telemanipulating from Guadalajara, Mexico, to Barcelona, Spain, using the Internet as the communication channel.

## 2. PREVIOUS WORKS

The applications of bilateral teleoperation systems span multiple areas, the most illustrative being space, underwater, medicine, and, in general, tasks with hazardous environments (Basañez and Suárez, 2009). The

⋆ This work was partially supported by the Spanish Government through the project DPI2016-80077-R and by the Mexican CONACyT Basic Scientific Research grant CB-282807.

reader may also refer to the work of Hokayem and Spong (2006) for an illustrative teleoperation historical survey.

One of the main problems in bilateral teleoperation control is that the communications exhibit time-delays and that these delays are, in general, time-varying (Nuño et al., 2009). Passivity has dominated the control schemes that deal with delays (Anderson and Spong, 1989; Stramigioli et al., 2002; Chopra et al., 2006; Secchi et al., 2008; Nuño et al., 2011; Hatanaka et al., 2015). Along this line Nuño et al. (2018) have reported one of the first controllers for bilateral teleoperators that ensures local-remote position tracking being robust to time-varying delays.

Since most of the commercially available robot hands do not incorporate velocity sensors, the scheme proposed by Nuño et al. (2018) is of special interest in the telemanipulation scenario because it ensures that position tracking is guaranteed without requiring velocity measurements.

In the teleoperation of anthropomorphic hand-arm systems, different interfaces have been used to capture the human input commands, as for instance, to capture the human arms movements: devices with accelerators (e.g. wiimotes) (Ciobanu et al., 2013) and magnetic trackers (Rosell et al., 2014); and to capture the human hands movements: tactile interfaces (Toh et al., 2012), video based systems (Ciobanu et al., 2013) and sensorized gloves (Rosell et al., 2014; Kukliński et al., 2014). Devices specifically designed to capture the finger movements and provide haptic feedback to the fingertips were also developed; for instance: the Phantom for a single finger (Massie and Salisbury, 1994), the MasterFinger for two fingers (Monroy et al., 2008), and the Hiro II (Halabi and Kawasaki, 2010) for five fingers but with only three degrees of freedom each of them.

When the operator has a full control of the remote robotic hand and commands it following his/her hand movements, the mapping of the human hand to the remote robotic hand plays a relevant role and can be done in different ways: a) joint-to-joint mapping, when each joint of the human hand is directly mapped to the corresponding joint of an anthropomorphic robotic hand (Kyriakopoulos et al., 1997); b) pose mapping, when the system identifies the pose of the human hand and moves the robotic hand to an equivalent preprogrammed pose (Kjellström et al., 2008); c) point-to-point mapping, when the positions of the human fingertip are identified and the fingertips of the robotic hand are commanded to equivalent ones (using inverse kinematics) (Peer et al., 2008), and d) hybrid systems that merge features of the previous ones (Colasanto et al., 2013).

When the operator shares the control with the remote robot, he/she does not need to access directly to the remote sensorial information, but can instead command the robot operation at a higher level and the remote system will react using the sensorial information and its own controllers (Griffin et al., 2005). The work presented in this paper follows this type of teleoperation. The unilateral telemanipulation strategy of Montaño and Suárez (2016, 2017) is extended here to bilateral telemanipulation.

The work of Salvietti et al. (2013) employs postural synergies obtained from a paradigmatic hand to control, using an intrinsically passive scheme, a robot hand. This scheme is also an example of a unilateral telemanipulation strategy where time-delays and human haptic feedback are not considered.

## 3. OVERVIEW OF THE PROPOSED APPROACH

This section provides a general overview of the proposed approach from the conceptual point of view.

The idea of this work is that the human operator uses a haptic device to command the movements that the robotic hand must perform to do the in-hand manipulation of an unknown object. Fig. 1 shows a diagram representing the main elements of the proposed system.

In the local station there are three main elements. A *Haptic Device* that, manipulated by the human operator, generates a vector $\boldsymbol{q}^l$ of joint values $q_i^l$, which is properly transformed into a vector with the desired configuration $\boldsymbol{\gamma}^l$ of the manipulated object by a *Forward Kinematics* module. $\boldsymbol{\gamma}^l$ is the information transmitted to the remote station through the communication channel. The third relevant block in the local station is the *Local Controller*, which is charge of generating the vector $\boldsymbol{\tau}_l$ of torques $\tau_{l_i}$ that the haptic device produces as a response to the human movements. The inputs to the Local Controller are two variables generated in the local station, $\boldsymbol{q}^l$ and $\boldsymbol{\gamma}^l$ plus two other variables received from the remote station, the object position $\boldsymbol{\gamma}^r(t-T^r(t))$ and the special binary signal $B(t-T^r(t))$ (explained below), with $T^r$ being the delay in the communication channel.

In the remote station there are four main elements, three of them equivalent, in some way, to those in the local station, and a special fourth element that plays a key role in the proposed approach. The first three elements are: a *Robotic Hand* whose configuration $\boldsymbol{q}^r$ is the vector of its joint values $q_i^r$, a *Forward Kinematics* module that uses $\boldsymbol{q}^r$ to compute the current configuration of the manipulated object $\boldsymbol{\gamma}^r$, and a *Remote Controller*, which is in charge of generating the vector of torques $\boldsymbol{\tau}_r$ that commands the robotic hand as a function of the error between its current configuration $\boldsymbol{q}^r$ and a setpoint $\boldsymbol{q}_d^r$. This setpoint $\boldsymbol{q}_d^r$ is generated by the special fourth element, called *Checker*, as a function of the error between $\boldsymbol{\gamma}^r$ and the commanded variable $\boldsymbol{\gamma}^l(t-T^l(t))$ received from the local station with a delay $T^l$. Basically, the Checker computes $\boldsymbol{q}_d^r$ using a manipulation strategy that tends to displace $\boldsymbol{\gamma}^r$ towards $\boldsymbol{\gamma}^l(t-T^l(t))$ with a reasonable small and tractable displacement that ensures the physical robustness of the grasp during the manipulation. Besides, since the object is unknown, it is not possible to predict the variation of the contact forces after each movement of the fingers and, for this reason, the potential increment o decrement of the grasping forces is also considered in the computation of $\boldsymbol{q}_d^r$, trying to keep the forces stable around a predefined value. The Checker is also in charge of detecting when a finger configuration is close to a joint limit as well as of predicting when a manipulation movement (computed according to the used manipulation strategy) may produce a grasping failure that makes the object to flip away or to fall down, because a grasping force reaches the limit of the friction cone. In order to communicate these situations to the local station, the Checker generates the binary signal $B$ that indicates

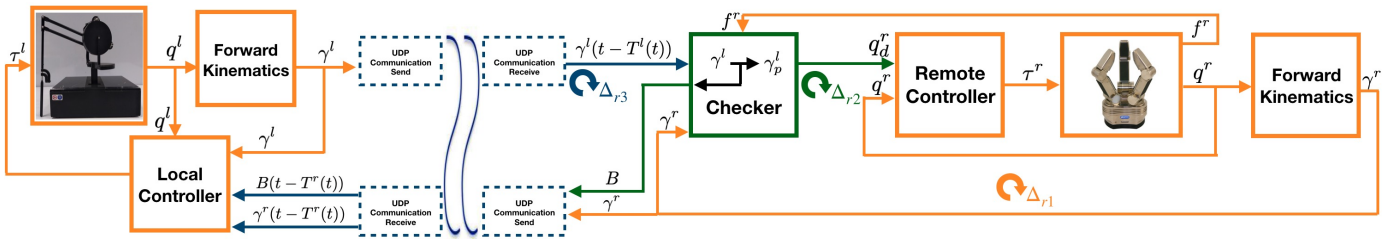


Fig. 1. Diagram of the proposed approach detailing the main elements and the relation between them.

whether the expected movement of the hand, computed to follow the command $\boldsymbol{\gamma}^l(t - T^l(t))$ received from the local station, is valid (safe and reachable) or not.

The elements mentioned above work within control loops with different frequencies, which must be taken into account for the correct operation of the whole system. The Remote Controller controls the hand actuators with a sampling period $\Delta_{r_1}$, but it receives the set-points from the Checker with a different period $\Delta_{r_2}$ and the Checker receives the information from the communication channel with a different sampling time $\Delta_{r_3}$.

In the next section, this approach is particularized for a specific type of manipulation and details of the particular implementation are also provided.

## 4. PARTICULAR IMPLEMENTATION AND EXPERIMENTAL VALIDATION

The proposed approach has been implemented with the particular goal of remotely commanding the rotation of an unknown grasped object around a predetermined axis. This type of manipulation is frequently done by human beings in daily tasks, for instance to inspect an object. The main features and assumptions of this particular implementation are:

1) The robotic hand uses only two fingers to grasp and rotate the object, as when the human being uses the thumb and index finger to hold and rotate an object.

2) The hand fingers are equipped with tactile sensors that allow the determination of the contact points on the fingertips and an estimation of the grasping force.

3) One degree of freedom of a haptic device in the local station is used to command the rotation of the grasped object in the remote station.

4) The grasping movements are outside the scope of this work. The telemanipulation is done starting with the object already hold by the two used fingers.

5) There is no knowledge about the shape or any other physical property of the manipulated object, like the center of mass. Nevertheless, it is assumed that the friction coefficient between the object and the fingertips is above an estimated value. This is a realistic assumption because, even when the object is unknown, the material of the fingertip is known and usually it has a large friction coefficient (like rubber or a similar materials).

In what follows, we describe the implementation of the proposed approach for the desired type of manipulation as well as the setup used in the real experimentation.

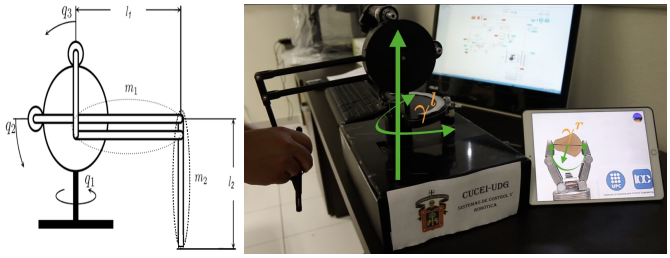

a) b)

Fig. 2. a) PHANTOM Premium 1.5 High Force haptic device diagram, and, b) testbed at local station located in Guadalajara, Mexico.


a) b)

Fig. 3. a) SDH2 hand with joint labels, b) testbed at the remote station located in Barcelona, Spain, with the SDH2 hand using two fingers opposite to each other to grasp an object.

### *4.1 Experimental setup*

For the validation of the proposed approach, transatlantic experiments have been carried on between the local station (Fig. 2) located at the Robotics lab of the CUCEI-UDG in Guadalajara, Mexico, and the remote station (Fig. 3) located at the Robotics lab of the IOC-UPC in Barcelona, Spain. The implementation makes use of C++, Matlab® and Simulink® version 8.1. The data transmission between the local and remote stations is done through UDP ports, and the main hardware is the following:

*Robotic hand.* This proposal uses the Schunk Dexterous Hand (SDH2), which is suitable for both, service robotics and industrial applications. SDH2 is a three-finger hand with tactile sensors attached to the surface of the fingertips and the proximal links. The hand has seven degrees of freedom, two for the flexion of each finger and an additional one that allows the coupled rotation of the base two fingers, allowing them to work opposite to each other (see Fig. 3b). A complete description of the hand

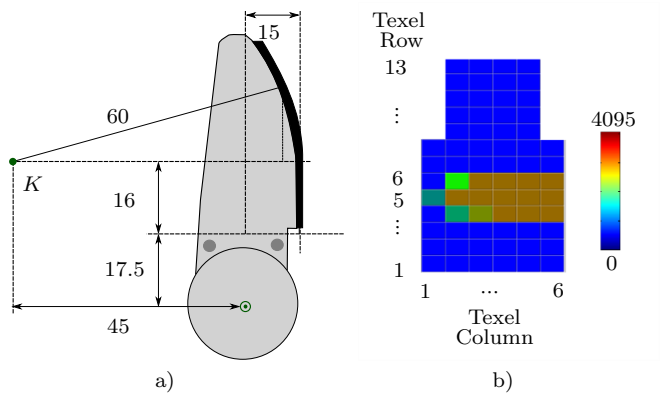


Fig. 4. a) Lateral view of a fingertip with the sensor pad, b) front representation of a fingertip sensor pad while contacting an object, the bar in the right indicates the scale of colors corresponding to the force values returned by each texel (all dimensions are in millimeters).

kinematics is given by Montaño and Suárez (2014). In this work, the fingertips of the two coupled fingers are used to grasp and manipulate an unknown object, performing a tip-pinch grasp (Feix et al., 2016). The tactile sensor pads on the fingertips have 68 sensitive texels split into two sections, a planar one that includes texel rows 1 to 5, with a wide of 6 texels, and a curved section that includes texels rows 6 to 13, with a wide of 6 texels from rows 6 to 8 and 4 texels from rows 9 to 13, as shown in Fig. 4. Each texel returns a value between 0 and 4095, corresponding, respectively, to 0 N when no pressure is applied, and 3 N when the maximum measurable normal force is applied over the texel. Surveys on the use of tactile sensors have been presented by Tegin and Wikander (2005) and Zou et al. (2017). The contact between a fingertip and the object takes place at a contact regions on the sensor pad, which may be composed of a single one or a set of disjoint subregions. The contact between each fingertip and the object is modeled using the punctual contact model (Nguyen, 1988), thus the barycenter of the actual contact region is considered as the current contact point, and the summation of the forces sensed at each texel in the actual contact region is considered as the current contact force $f_{i_k}$, $i = 1, 2$ applied by finger $i$ at the equivalent punctual contact (Wörn and Haase, 2012).

*Haptic device.* A PHANTOM Premium 1.5 High Force® (Fig. 2) is employed in the experimental validation. It provides three degrees of freedom with positional sensing and force feedback. This device is commercially available from 3D SYSTEMS®. The communication at the local station between Simulink® and the haptic is done using the homemade library *PhanTorque_3Dof* [1]

### *4.2 Local station*

As shown in Fig. 1, the local station has three elements, namely: a haptic device; a Forward Kinematics module; and the Local Controller. The haptic PHANTOM Premium, described above, works together with a computer and only one degree of freedom, that is $q_1$, is used to command the object rotation $\gamma^l$. For this reason the Forward Kinematics module is straightforward, and only a scaling factor is introduced to take advantage of the haptic device workspace, establishing the relation between these variables as $\gamma^l = 0.4q^l$.

Regarding the Local Controller, it is implemented in Simulink according to the following control law (Aldana et al., 2018),

$$\tau^l = -k^l \left(\gamma^l - \theta^l\right), \tag{1}$$

where the gain $k^l$ is any positive number and $\theta^l$ stands for the generalized coordinate of the controller, that is obtained by solving the following second order ordinary-differential-equation

$$\ddot{\theta}^l = -k^l(\theta^l - \gamma^l) - d^l\dot{\theta}^l - p^l(\theta^l - \gamma^r(t - T^r(t))) \tag{2}$$

where $d^l, p^l > 0$ are the damping and the proportional gains.

Since the SDH2 hand does not allow the user to set a desired torque, the Remote Controller is implemented as a set-point position-based scheme that works with the proprietary SDH2 hand controller. In this work we assume that such controller is a simple proportional plus damping scheme with control gains approximately equal to those of the Local Controller. Therefore, we assume that $d^l = d^r$ and $p^l = p^r$. In order for the controller to be robust to time-delays, the control gains have to satisfy

$$d^l > \tfrac{1}{2}({}^*T^l + {}^*T^r)p^l, \tag{3}$$

where ${}^*T^l$ and ${}^*T^r$ are the bounds of the time-delays (Aldana et al., 2018).

Without requiring velocity measurements and provided that sufficiently large damping is injected, i.e. (3) holds, this scheme guarantees that $\lim_{t\to\infty} \gamma^l(t) - \gamma^r(t) = 0$ (Aldana et al., 2018; Nuño et al., 2018).

### *4.3 Remote station*

The main element of the remote station is the Checker, which has two main duties: a) compute the setpoint $\boldsymbol{q}_d^r$ for the Remote Controller to move the hand fingers according to the information received from the local station; and, b) generate the binary signal $B$ when the computed setpoint is not reachable because the fingers reach one or more joint limits, or the grasping forces are close to reach the limits of the friction cone and therefore the object could fall down or flip away.

Duty (a) is solved as follows. Let the subscript $k$ represent the value of the variables in the $k$ iteration. First, the current state of the grasp is determined by computing the current absolute positions of the contact points $\boldsymbol{P}_{i_k}$, $i = 1, 2$ and the current grasping forces $f_{i_k}$. $\boldsymbol{P}_{i_k}$, $i = 1, 2$ are directly computed using the tactile information to identify the contact points on the sensor pads and the hand forward kinematics (FK). In the case of a two-finger grasp, the contact forces $f_{i_k}$ should have the same magnitude and opposite direction, but due to different sources of uncertainties and measurement errors this may not be exactly true. In order to minimize errors, $f_{i_k}$, $i = 1, 2$ are considered to have the right direction and a magnitude $f_k$ equal to the average of the measured values at each fingertip.

[1] The library is publicly available at:
http://sir.upc.edu/wikis/roblab/index.php/Projects/PhanTorqueLibraries

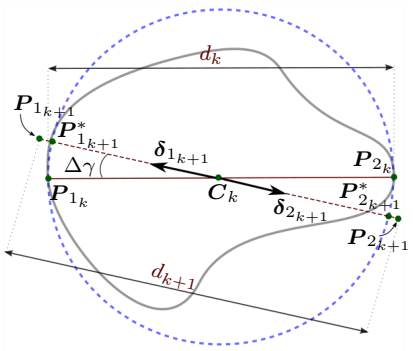


Fig. 5. Example of computation of $\boldsymbol{P}_{i_{k+1}}$ using the auxiliary points $\boldsymbol{P}^*_{i_{k+1}}$ and the adjustment of the distance $d_k$.

Then, new contact points $\boldsymbol{P}_{i_{k+1}}$ are computed aiming for a proper object rotation and adjustment of $f_{k+1}$.

Let us consider the Euclidean distance between contact points $\boldsymbol{P}_{i_k}$, $i = 1, 2$, and the middle point $\boldsymbol{C}_k$ between them, i.e.

$$d_k = \sqrt{(\boldsymbol{P}_{1_{k_x}} - \boldsymbol{P}_{2_{k_x}})^2 + (\boldsymbol{P}_{1_{k_y}} - \boldsymbol{P}_{2_{k_y}})^2} \tag{4}$$

$$\boldsymbol{C}_k = \frac{\boldsymbol{P}_{2_k} - \boldsymbol{P}_{1_k}}{2} + \boldsymbol{P}_{1_k} \tag{5}$$

Now, two auxiliary contact points $\boldsymbol{P}^*_{i_{k+1}}$ are computed by displacing $\boldsymbol{P}_{i_k}$ along a circular path with diameter $d_k$ and centered in $\boldsymbol{C}_k$, as shown in Fig. 5, i.e.

$$P^*_{1_{k+1_x}} = C_{k_x} - (d_k/2)\cos(\phi + s_r\Delta\gamma) \tag{6}$$

$$P^*_{1_{k+1_y}} = C_{k_y} - (d_k/2)\sin(\phi + s_r\Delta\gamma) \tag{7}$$

$$P^*_{2_{k+1_x}} = C_{k_x} + (d_k/2)\cos(\phi + s_r\Delta\gamma) \tag{8}$$

$$P^*_{2_{k+1_y}} = C_{k_y} + (d_k/2)\sin(\phi + s_r\Delta\gamma) \tag{9}$$

where $\Delta\gamma$ is an empirical value chosen small enough to assure small movements of the object on each manipulation step $k$, and $s_r$ depends on the difference between the current object orientation $\boldsymbol{\gamma}^r$ (computed in the remote station) and the desired orientation $\boldsymbol{\gamma}^l(t - T^l(t))$ (received from the local station), as

$$s_r = -\tanh(\boldsymbol{\gamma}^r - \boldsymbol{\gamma}^l(t - T^l(t))) \tag{10}$$

Note that the direction of the displacement of $\boldsymbol{P}^*_{i_{k+1}}$ with respect to $\boldsymbol{P}_{i_k}$ corresponds to the desired sense of rotation of the object given by the sign of $\boldsymbol{\gamma}^r - \boldsymbol{\gamma}^l(t - T^l(t))$.

Since the shape of the object is unknown, any finger movement may alter the grasping force $f_k$, which must remain within a threshold around a desired value $f_d$ (if $f_k$ increases a lot the object or the hand may be damaged and if $f_k$ decreases the grasp may fail and the object may fall down), i.e. the manipulation must try to minimize the force error

$$e_k = f_k - f_d \tag{11}$$

During the manipulation, in each iteration, $f_k$ is adjusted by adjusting $d_k$ as

$$d_{k+1} = d_k + \Delta d_k \tag{12}$$

with $\Delta d_k$ depending on $e_k$ as

$$\Delta d_k = \begin{cases} 2\lambda(\|e_k\| + {e_k}^2) & \text{if } e_k \leq 0 \\ -\lambda e_k & \text{if } e_k > 0 \end{cases} \tag{13}$$

being $\lambda$ a predefined constant, empirically obtained. The reason for the different gain depending on the sign of $e_k$ is that a potential fall of the object ($f_{i_k} \to 0$) is considered more critical that a potential application of large grasping forces ($f_{i_k} \gg f_d$).

The next (expected) contact points $\boldsymbol{P}_{i_{k+1}}$ that intend to change the object orientation $\boldsymbol{\gamma}^r$ and also adjust the force $f_k$, are computed as,

$$\boldsymbol{P}_{i_{k+1}} = \boldsymbol{C}_k + \frac{d_{k+1}}{2}\boldsymbol{\delta}_{i_{k+1}} \tag{14}$$

where $\boldsymbol{\delta}_{i_{k+1}}$ is the unitary vector from $\boldsymbol{C}_k$ to $\boldsymbol{P}^*_{i_{k+1}}$ (see Fig. 5).

Finally, the hand configuration $\boldsymbol{q}^r_{d_{k+1}}$ is obtained from the points $\boldsymbol{P}_{i_{k+1}}$ directly using the inverse kinematics of the fingers, i.e. $\boldsymbol{q}^r_{d_{k+1}} = \text{IK}(\boldsymbol{P}_{1_{k+1}}, \boldsymbol{P}_{2_{k+1}})$.

Duty (b) of the Checker is solved as follows. We will consider $B = 0$ when $\boldsymbol{q}^r_{d_{k+1}}$ is reachable and safe to keep the grasp, and therefore the manipulation movement can be actually done, or $B = 1$ otherwise. Determining whether $\boldsymbol{q}^r_{d_{k+1}}$ is reachable is straightforward, it simply means that $\boldsymbol{q}^r_{d_{k+1}} = \text{IK}(\boldsymbol{P}_{1_{k+1}}, \boldsymbol{P}_{2_{k+1}})$ returns a valid hand configuration. Determining whether $\boldsymbol{q}^r_{d_{k+1}}$ produces a safe grasp is done by checking whether the expected applied force $f_{i_{k+1}}$ lies inside the friction cone. As stated above, the grasping forces $f_{i_{k+1}}$ are aligned with the segment defined by $\boldsymbol{P}_{1_{k+1}}$ and $\boldsymbol{P}_{2_{k+1}}$, so their directions are known, and the direction $\hat{n}_i$ normal to each fingertip at $\boldsymbol{P}_{1_{k+1}}$ is also known (the shape of the fingertip is known). Then, if the angle $\beta_i$ between $f_{i_{k+1}}$ and $\hat{n}_i$ is smaller that the angle of the friction cone, $\alpha = \arctan(\mu)$ being $\mu$ the friction coefficient, then the grasp can be considered safe, i.e. $B = 0$ if $\beta_i < \alpha$. Note that the actual friction coefficient is not known, neither explicitly computed during the manipulation, thus, a given minimum value is assumed in order to determine $B$. This is a reasonable assumption, since the material of the fingertips (rubber) is known and it produces a reasonable $\mu$ for most of the unknown manipulated objects. Algorithm 1 summarizes the steps done by the Checker.

Another element of the remote station is the FK module, which is in charge of computing the current orientation of the object $\boldsymbol{\gamma}^r$ from the current configurations of the fingers $\boldsymbol{q}^r_{k+1}$. Since the object is unknown, after finger movements this transformation cannot be fully determined without using external sensors (like, for instance, a vision system), but, as shown by Montaño and Suárez (2018), it can be estimated with enough precision using the following expression initially proposed for fingertips with circular shape (Ozawa et al., 2004),

$$\boldsymbol{\gamma}^r \approx \frac{R}{d_k}\left(\sum_{j=1}^{n_1}(q_{1j_{\gamma_0}} - q_{1j_k}) - \sum_{j=1}^{n_2}(q_{2j_{\gamma_0}} - q_{2j_k})\right) \tag{15}$$

where:

$q_{ij_k}$ is the current value of joint $j$ of finger $i$,
$q_{ij_{\gamma_0}}$ is the value of joint $j$ of finger $i$ at the initial grasp,
$d_k$ is the distance between the contact points, and
$R$ is the radius of the fingertip (R = 60 mm for the SDH2).

**Algorithm 1** Steps done in the Checker.

**Require:** $f_{i_k}$, $f_d$, $\boldsymbol{\gamma}^r$, $\boldsymbol{\gamma}^l(t - T^l(t))$
**Ensure:** $\boldsymbol{q}^r_{k+1}$, $B$

**procedure** CHECKER
  $k \leftarrow 0$
  **loop**
    Check for new values of $\boldsymbol{\gamma}^l(t - T^l(t))$
    Compute $\boldsymbol{P}_{i_k}$ using FK
    Compute $f_k$
    Compute $d_k$ using (4)
    Compute $\boldsymbol{P}^*_{i_{k+1}}$ using (6 to 9)
    Compute $d_{k+1}$ using (12)
    Compute $\boldsymbol{P}_{i_{k+1}}$ using (14)
    Compute $\boldsymbol{q}^r_{k+1}$ using IK($\boldsymbol{P}_{1_{k+1}}$,$\boldsymbol{P}_{2_{k+1}}$)
    **if** $\boldsymbol{q}^r_{k+1}$ is reachable and safe **then**
      Send $\boldsymbol{q}^r_{k+1}$ to *Remote Controller*
      $B \leftarrow 0$
    **else**
      $B \leftarrow 1$
    **end if**
    Send $B$ to *local station*
    $k \leftarrow k + 1$
  **end loop**
**end procedure**

### *4.4 Experimental results*

The grasped object shown in Fig. 3b is used in the experiments described below, using the following gains and parameters. At the local station the Local Controller gains are $k^l = 15$, $d^l = 8$ and $p^l = 2$. At the remote station (checker) the desired grasping force is set to $f_d = 5$ N, the constant to adjust the distance between contact points is set to $\lambda = 0.1$, the constant $\Delta\gamma$ is set to 0.25 degrees, and the minimum friction coefficient is assumed to be $\mu = 0.4$ (i.e. $\alpha \approx 0.38$ rad).

Fig. 6 shows the orientation of the object ($\boldsymbol{\gamma}^r$) and the desired orientation ($\boldsymbol{\gamma}^l$) commanded by the local operator through the first joint of the haptic device. It can be observed that the object follows the desired orientation and, when it is pushed to perform a non valid movement, it keeps the current orientation until a valid movements is demanded, this effect can be clearly appreciated in the intervals: 12s to 22s, 38s to 48s and 65s to 72s. Fig. 7 shows the torque applied to the haptic device and the behavior of the binary signal $B$. It can be observed that when the non-valid movement signal is received (i.e. $B = 1$), an increasing torque is applied to the haptic device emulating a wall for the local operator, this allows the local operator to realize that the movement of the object is reaching a limit. Fig. 8 shows the friction cone angle $\alpha$ and the angles $\beta_1$ and $\beta_2$ that indicate whether the movement defined by $\boldsymbol{q}^r_{k+1}$ is safe. When $\|\beta_1\|$ and $\|\beta_2\|$ are smaller than $\|\alpha\|$, the binary signal $B = 0$ indicates to the local station that the movement can be executed safely. Fig. 9 shows the grasping force $f_k$ and the desired force $f_d$. The variable time-delay between the local and remote stations along the experiment can be observed in Fig. 10, for which ${}^*T^l = {}^*T^r = 0.65$ s.

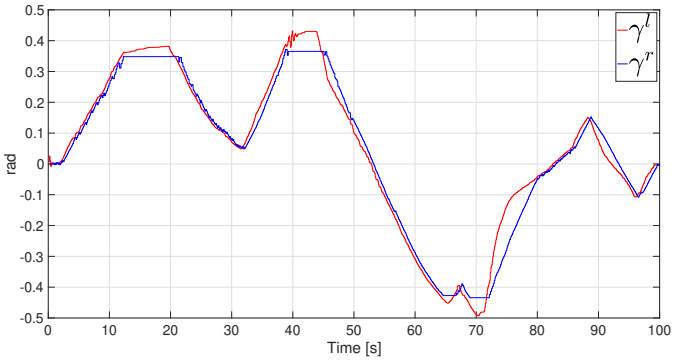


Fig. 6. Local orientation $\gamma^l$ and remote object orientation $\gamma^r$.

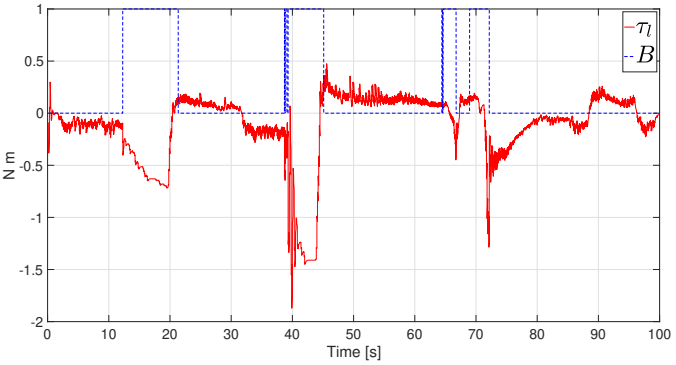


Fig. 7. Local torque $\tau^l$ and the signal $B$ indicating valid ($B = 0$) and non valid ($B = 1$) movements.

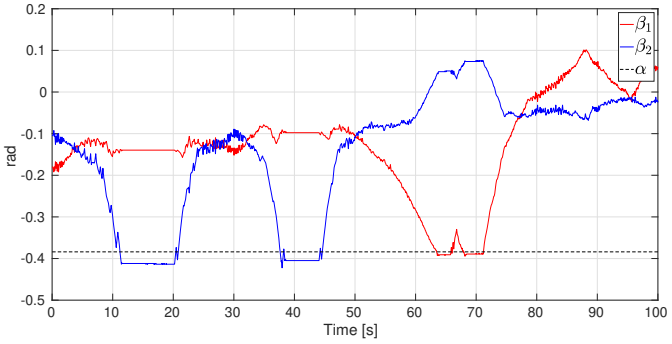


Fig. 8. Angles $\beta_1$ and $\beta_2$, and the friction cone $\alpha$.

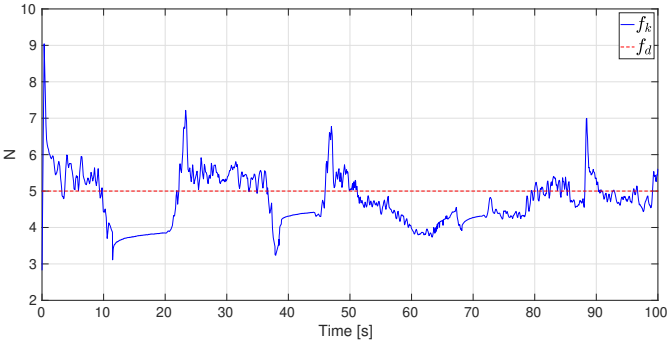


Fig. 9. Grasping force $f_k$ and desired force $f_d$.

Figs. 11 to 14 show the results of a second experiment [2] (the variable time-delays are similar to those shown in Fig. 10 so they are not included). Note that in this case

[2] A video showing the system performance can be found in: https://sir.upc.edu/projects/dexterous_telemanipulation/index.html Fig. 3b shows a snapshot of the execution.

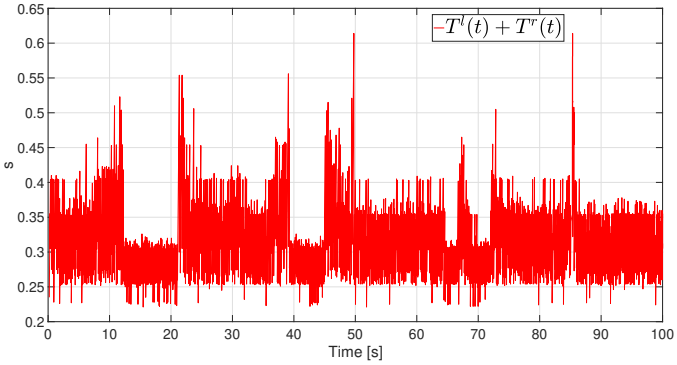


Fig. 10. Time-delay in the communication channel $T^l + T^r$.

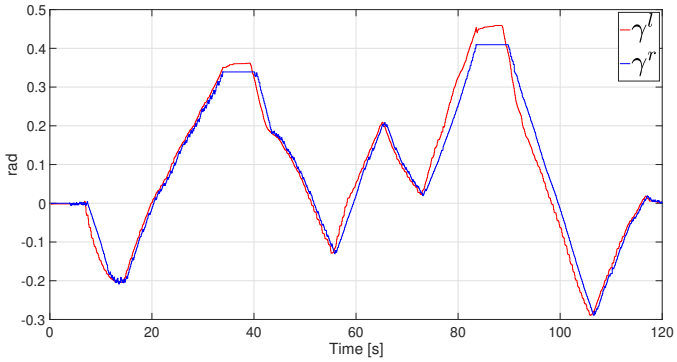


Fig. 11. Local orientation $\boldsymbol{\gamma}^l$ and remote object orientation $\boldsymbol{\gamma}^r$.

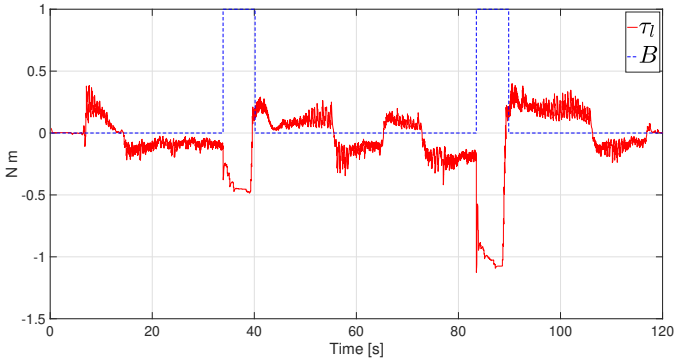


Fig. 12. Local torque $\tau^l$ and the signal $B$ indicating valid ($B = 0$) and non valid ($B = 1$) movements.

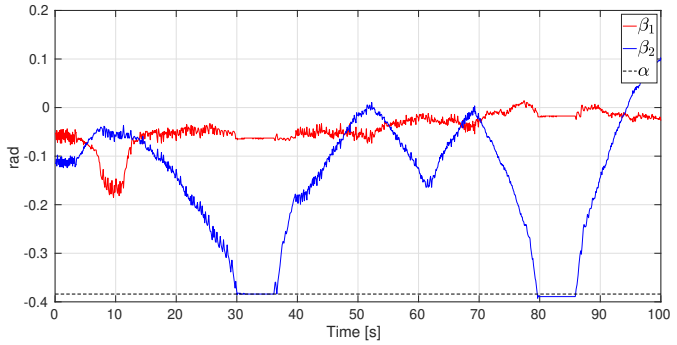


Fig. 13. Angles $\beta_1$ and $\beta_2$, and the friction cone $\alpha$.

the local operator demands twice a non-valid movement, in the intervals 34s to 40s and 85s to 90s.

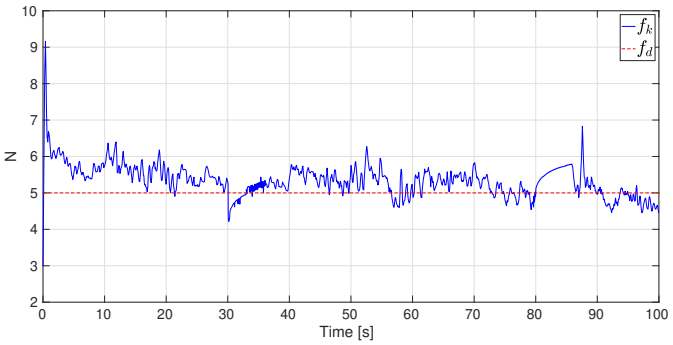


Fig. 14. Grasping force $f_k$ and desired force $f_d$.

## 5. CONCLUSIONS AND FUTURE WORK

This paper has presented a shared control scheme for bilateral in-hand dexterous telemanipulation with variable time-delays in the communication channel. On the one hand, our novel proposal employs tactile and kinematic information to manipulate an unknown object with the commanded orientation given remotely by a human operator that might be located far away. On the other hand, the human operator receives force feedback information regarding the object manipulation and the feasibility of the commanded movements. Real telemanipulation experiments between Guadalajara, Mexico, and Barcelona, Spain, demonstrate the effectiveness of the proposal.

Future research avenues are twofold: the use of more than two fingers of a force-controlled hand and the integration of the in-hand object telemanipulation with the teleoperation of the robotic arm.

## REFERENCES

Aldana, C.I., Cruz, E., Nuño, E., and Basañez, L. (2018). Control in the operational space of bilateral teleoperators with time-delays and without velocity measurements. *IFAC-PapersOnLine*, 51(13), 204–209.

Anderson, R.J. and Spong, M.W. (1989). Bilateral control of teleoperators with time delay. *IEEE Transactions on Automatic Control*, 34(5), 494–501.

Basañez, L. and Suárez, R. (2009). Teleoperation. In *Nof S. (eds) Springer Handbook of Automation. Springer Handbooks*, 449–468. Springer Berlin Heidelberg.

Chopra, N., Spong, M.W., Ortega, R., and Barabanov, N. (2006). On tracking performance in bilateral teleoperation. *IEEE Transactions on Robotics*, 22(4), 861–866.

Ciobanu, V., Popescu, N., Petrescu, A., and Noeske, M. (2013). Robot telemanipulation system. In *17th International Conference on System Theory, Control and Computing (ICSTCC 2013)*, 681–686.

Colasanto, L., Suárez, R., and Rosell, J. (2013). Hybrid mapping for the assistance of teleoperated grasping tasks. *IEEE Transactions on Systems, Man, and Cybernetics Part A: Systems and Humans*, 43(2), 390–401.

Feix, T., Romero, J., Schmiedmayer, H.B., Dollar, A.M., and Kragic, D. (2016). The GRASP Taxonomy of Human Grasp Types. *IEEE Transactions on Human-Machine Systems*, 46(1), 66–77.

Griffin, W.B., Provancher, W.R., and Cutkosky, M.R. (2005). Feedback strategies for telemanipulation with shared control of object handling forces. *Presence: Teleoperators and Virtual Environments*, 14(6), 720–731.

Halabi, O. and Kawasaki, H. (2010). Five Fingers Haptic Interface Robot HIRO: Design, Rendering, and Applications. In M.H. Zadeh (ed.), *Advances in Haptics*, 221–240. InTech.

Hatanaka, T., Chopra, N., Fujita, M., and Spong, M.W. (2015). *Passivity-based control and estimation in networked robotics*. Communications and Control Engineering. Springer, Cham.

Hokayem, P.F. and Spong, M.W. (2006). Bilateral teleoperation: An historical survey. *Automatica*, 42(12), 2035–2057.

Kjellström, H., Romero, J., and Kragić, D. (2008). Visual recognition of grasps for human-to-robot mapping. In *IEEE/RSJ 2008 International Conference on Intelligent Robots and Systems (IROS 2008)*, 3192–3199.

Kukliński, K., Fischer, K., Marhenke, I., Kirstein, F., aus der Wieschen, M.V., Sølvason, D., Krüger, N., and Savarimuthu, T.R. (2014). Teleoperation for learning by demonstration: Data glove versus object manipulation for intuitive robot control. In *2014 6th International Congress on Ultra Modern Telecommunications and Control Systems and Workshops (ICUMT)*, 346–351.

Kyriakopoulos, K.J., Van Riper, J., Zink, A., and Stephanou, H.E. (1997). Kinematic analysis and position/force control of the Anthrobot dextrous hand. *IEEE Transactions on Systems, Man, and Cybernetics, Part B: Cybernetics*, 27(1), 95–104.

Massie, T.H. and Salisbury, K.J. (1994). PHANToM haptic interface: a device for probing virtual objects. In *American Society of Mechanical Engineers, Dynamic Systems and Control Division*, 295–301. American Society of Mechanical Engineers (ASME).

Monroy, M., Ferre, M., Campos, A., Barrio, J.J., and Oyarzabal, M. (2008). MasterFinger: Multi-finger Haptic Interface for Collaborative Environments. In *Haptics: Perception, Devices and Scenarios*, 411–419. Springer Berlin Heidelberg.

Montaño, A. and Suárez, R. (2014). Getting comfortable hand configurations while manipulating an object. In *19th IEEE International Conference on Emerging Technologies and Factory Automation (ETFA'14)*, 1–8.

Montaño, A. and Suárez, R. (2016). Commanding the Object Orientation Using Dexterous Manipulation. In L. Reis, A. Moreira, P. Lima, L. Montano, and V. Muñoz-Martinez (eds.), *Robot 2015: Second Iberian Robotics Conference. Advances in Intelligent Systems and Computing*, volume 418, 69–79. Springer, Cham.

Montaño, A. and Suárez, R. (2017). Robust dexterous telemanipulation following object-orientation commands. *Industrial Robot: An International Journal*, 44(5), 648–657.

Montaño, A. and Suárez, R. (2018). Manipulation of Unknown Objects to Improve the Grasp Quality Using Tactile Information. *Sensors*, 18(5), 1412.

Nguyen, V.D. (1988). Constructing Force- Closure Grasps. *The International Journal of Robotics Research*, 7(3), 3–16.

Nuño, E., Arteaga-Pérez, M., and Espinosa-Pérez, G. (2018). Control of bilateral teleoperators with time delays using only position measurements. *International Journal of Robust and Nonlinear Control*, 28(3), 808–824.

Nuño, E., Basañez, L., and Ortega, R. (2011). Passivity-based control for bilateral teleoperation: A tutorial. *Automatica*, 47(3), 485–495.

Nuño, E., Basañez, L., Ortega, R., and Spong, M.W. (2009). Position Tracking for Non-linear Teleoperators with Variable Time Delay. *The International Journal of Robotics Research*, 28(7), 895–910.

Ozawa, R., Arimoto, S., Nguyen, P.T.A., Yoshida, M., and Bae, J.H. (2004). Manipulation of a circular object in a horizontal plane by two finger robots. In *2004 IEEE International Conference on Robotics and Biomimetics (ROBIO 2004)*, 517–522.

Peer, A., Einenkel, S., and Buss, M. (2008). Multi-fingered telemanipulation - Mapping of a human hand to a three finger gripper. In *17th IEEE International Symposium on Robot and Human Interactive Communication (RO-MAN 2008)*, 465–470.

Rosell, J., Suárez, R., and Pérez, A. (2014). Safe teleoperation of a dual hand-arm robotic system. In M. Armada, A. Sanfeliu, and M. Ferre (eds.), *ROBOT2013: First Iberian Robotics Conference. Advances in Intelligent Systems and Computing*, volume 253, 615–630. Springer, Cham.

Salvietti, G., Wimböck, T., and Prattichizzo, D. (2013). A Static Intrinsically Passive Controller to Enhance Grasp Stability of Object-based Mapping between Human and Robotic Hands. In *IEEE/RSJ 2013 International Conference on Intelligent Robots and Systems (IROS 2013)*, 2460–2465.

Secchi, C., Stramigioli, S., and Fantuzzi, C. (2008). Transparency in Port-Hamiltonian-Based Telemanipulation. *IEEE Transactions on Robotics*, 24(4), 903–910.

Stramigioli, S., van der Schaft, A., Maschke, B., and Melchiorri, C. (2002). Geometric scattering in robotic telemanipulation. *IEEE Transactions on Robotics and Automation*, 18(4), 588–596.

Tegin, J. and Wikander, J. (2005). Tactile sensing in intelligent robotic manipulation a review. *Industrial Robot: An International Journal*, 32(1), 64–70.

Toh, Y.P., Huang, S., Lin, J., Bajzek, M., Zeglin, G., and Pollard, N.S. (2012). Dexterous telemanipulation with a multi-touch interface. In *2012 12th IEEE-RAS International Conference on Humanoid Robots (Humanoids 2012)*, 270–277.

Wörn, H. and Haase, T. (2012). Force approximation and tactile sensor prediction for reactive grasping. In *2012 World Automation Congress*, 1–6.

Zou, L., Ge, C., Wang, Z., Cretu, E., and Li, X. (2017). Novel Tactile Sensor Technology and Smart Tactile Sensing Systems: A Review. *Sensors*, 17(11), 2653.